

# Development and Evaluation of the Mechanical Properties of Coconut Fibre Reinforced Low Density Polyethylene Composite

Ahmed Mohammed Bukar, Abubakar Mohammed El-Jumrah, Abba Alhaji Hammajam

Department of Mechanical Engineering, University of Maiduguri, Maiduguri, Nigeria

Email: hammajam92@gmail.com

**How to cite this paper:** Bukar, A.M., El-Jumrah, A.M. and Hammajam, A.A. (2022) Development and Evaluation of the Mechanical Properties of Coconut Fibre Reinforced Low Density Polyethylene Composite. *Open Journal of Composite Materials*, 12, 83-97.

<https://doi.org/10.4236/ojcm.2022.123007>

**Received:** April 5, 2022

**Accepted:** June 14, 2022

**Published:** June 17, 2022

Copyright © 2022 by author(s) and Scientific Research Publishing Inc.

This work is licensed under the Creative Commons Attribution-NonCommercial International License (CC BY-NC 4.0).

<http://creativecommons.org/licenses/by-nc/4.0/>



Open Access

## Abstract

This research work developed and evaluated the mechanical properties of coconut fibre reinforced low density polyethylene (LPDE) composite material. The effect of fibre loading on the mechanical properties: tensile, flexural, and impact of the developed composite material have been investigated. Also carried out was the effect of fibre loading on the water absorptivity of the developed material. Sample categories of the developed composite were prepared by varying the fibre contents by weight at 0%, 10%, 20%, and 30%. The aim is to reduce the excessive waste disposal of LDPE materials that are largely found in the form of disposed water package materials (or pure water sachets) that usually affects the environment in the form of pollution. The water retting process was applied in extracting and cleaning fibre (or coir), while the mixed coir-LDPE (or developed composite material) was prepared by Compression Moulding Technique (CMT). The tensile and flexural properties were tested using Hounsfield Monsanto Tensometer (type w) while the impact properties were tested using the Charpy Impact testing machine. The microstructure of the composite was investigated using Scanning Electron Microscopy (SEM). The fractured surface morphology of the composite samples indicated a homogeneous mixture of the coir fibre and LDPE matrix. However, weak interfacial bonding between the coir fibre and LDPE matrix was also observed. The analysis of the water absorptivity showed that the developed composite materials have low water absorptivity at low fibre loading. However, at higher fibre loading, the water absorptivity increases significantly.

## Keywords

Coconut Fibre, Low Density Polyethylene, Composite, Mechanical Properties, Water Absorptivity

## 1. Introduction

Composites are multifunctional materials consisting of two or more chemically distinct constituents, having a distinct interface separating them. The discontinuous phase is embedded in a continuous phase to form the composite. Natural fibres have been applied as reinforcement in composite materials; related to this project, Coir fibre is employed as the reinforcement due to its availability and its rich fibrous mesocarp, which is a resource for fibres that can be used in fibre reinforced composites as a reinforcing material. The role of fibres in a composite material is to provide a framework of support and strength to the weak polymer matrix. In order to attain a set of desirable properties, the fibres must consist of properties such as high elastic modulus, good stiffness and compressive strengths, etc. [1].

This work was informed by the need for the development of a cheap method of obtaining composite material with acceptable properties and characteristics. The study is an attempt to solve the key environmental problems related to the disposal of solid waste (LDPE) and agricultural waste (Coir fibre) in the environment. In addition, the use of natural fibres from agricultural wastes is also in conformity with the re-use and re-utilization of growing agricultural wastes. Furthermore, the major disadvantage relating to the use of composite materials is their high-cost demand. From a problem-solving perspective, these are not worthy. Thus, there is a need to develop a cheap method of obtaining composite material and a way of reducing the amount of waste in the environment, judging from both material recycling and environmental protection viewpoint.

The coir fibre was used as a reinforcing material by man not long ago compared to other natural fibres. However, the development of coir fibre in composites has recently gained attention due to its low cost, easy availability, low density, ease of separation, biodegradability, and recyclable in nature [2]. One of the earliest use of coir in FRP composites was found in the production of automobile parts [3]. According to the author of the study, recent investigations have shown that coconut and other fruit fibres possess acceptable mechanical properties for application in the production of low-priced FRP composites. [4] investigated the possibility of the introduction of natural fibres (Coconut fibres, basalt fibres, and wood flour) as a hybrid reinforcement of bio-polyethylene composites. The result showed that the use of natural fibre as filler in a hybrid reinforced bio-polyethylene composite increased the rigidity and strength properties of polyethylene. [5] investigated the suitability of Coconut fibre reinforced polymer composite for the production of a military helmet. The results obtained indicated that the coconut fibre enhanced the impact strength of the polymer. The authors concluded that coir fibre can be used comfortably as reinforcement in polymer matrix composite for the production of Military helmets.

## 2. Materials and Methods

### 2.1. Materials

The matrix material used in this work is the thermoplastic low density polyethy-

lene (LDPE) material shown in **Figure 1(a)**. Its density is in the range of 0.91 - 0.94 g/cm<sup>3</sup>, it is stable at a temperature ranging from -50°C to 85°C and melts at a temperature of about 115°C [6]. The LDPE in addition to mixing with the fibre, also surrounds the fibre to complete the development process of the composite material.

The fibre materials as shown in **Figure 1(b)** are the reinforcing medium, which are extracts from the mesocarp of coconut fruit known as coir. The coir fibre consist of the fine yarns of diameters ranging from 0.152 mm to 0.635 mm which was measured using the Moore and Wright micrometer screw gauge (FE Teaching Workshop, University of Maiduguri). It has density of 1.2 g/cm<sup>3</sup>, tensile strength of 175 MPa and water absorption ranging from 130% - 180% [7].

The material that was used to construct the metallic mould is mild steel. It has tensile strength of 440 MPa, thermal conductivity of 54 W/mK and melting point ranging from 1350°C - 1530°C. The selection of this material is based on the fact that it is capable of dissipating heat rapidly since it has high thermal conductivity, thus, allowing the moulded composite to cool rapidly without buckling. The mould was constructed from 3 mm thick mild steel sheet in the form of a square plate mould and the dimension of the mould is 250 × 250 mm from which the cavity of 150 × 150 mm was perforated as shown in **Figure 1(c)**.

## 2.2. Methods

### 2.2.1. Fibre Extraction and Cleaning

The coir fibre was extracted from the coconut husks obtained using the water rating process as shown in **Figure 2**. The process involves the soaking of the coconut husk in water for a period of 2 days to soften the bond between the exocarp & the mesocarp (coir) and separate them. The coir obtained was then soaked again in water for a period of 5 days to soften the hard coir. The extracted fibres were cleaned by beating off the husks lightly until the pithy substances were removed. Dewaxing of the fibre by boiling and subsequently soaking in hot detergent for 1 hour was done. The fibres were then rinsed and sun dried for the period of 8 - 10 hours. After drying, the fibres were stored in polyethylene bags.

### 2.2.2. Sample Preparation

The composite material was developed based on the percentage by weight

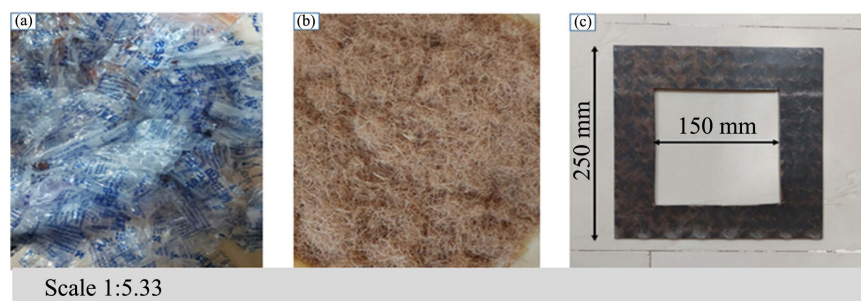


**Figure 1.** Materials, (a) LDPE matrix; (b) Coir fibre; (c) Mild steel mould.

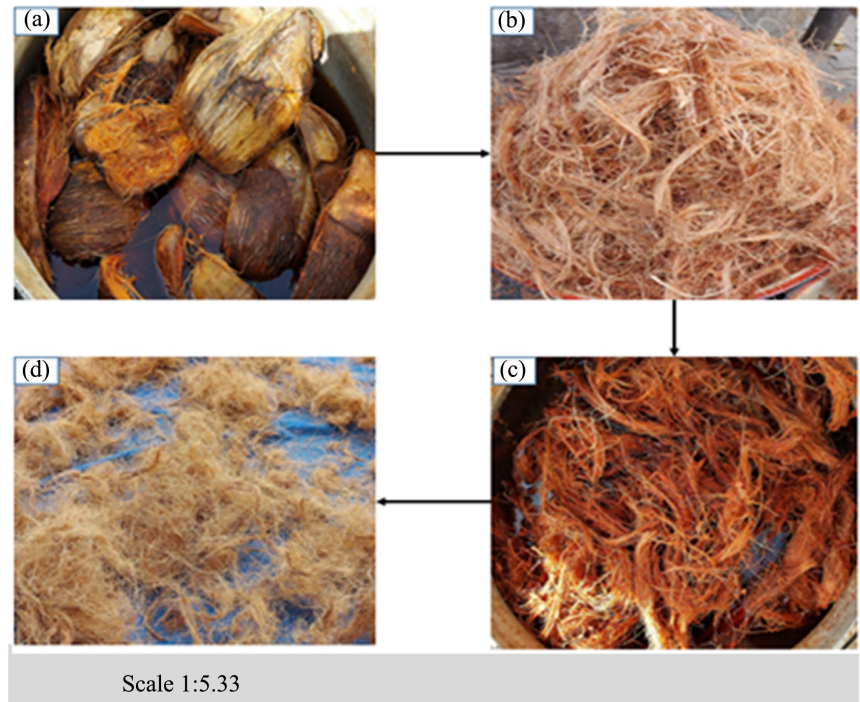


**Figure 2.** Fibre extraction and cleaning, (a) Soaked coconut; (b) Separated mesocarp (coir) from the exocarp; (c) Soaked coir; (d) Sun dried coir.

mixture of coconut fibre and LDPE, which were categorized into 0, 10, 20, 30 and 40 wt% of the coconut fibre and 100, 90, 80, 70 and 60 wt% of the LDPE. The measurement of the samples was based on information obtained on the physical properties of the matrix and the fibre. These include density, volume, mass and fibre volume fraction. The weight of the test samples was measured manually using digital weighing scale, but the equivalent fibre weight fraction was obtained using the laminate formulae.

Fibre Volume Fraction (FVF) from Fibre Weight Fraction (FWF).

$$FVF = \frac{1}{1 + \frac{\rho_f}{\rho_m} \left( \frac{1}{FWF} - 1 \right)} \tag{1}$$

Fibre Weight Fraction (FWF) from Fibre Volume Fraction (FVF).

$$FWF = \frac{\rho_f \times FVF}{\rho_m + (\rho_f - \rho_m) \times FVF} \tag{2}$$

From **Equation (2)**, for FVF = 10%, 20%, 30%, and 40%, the equivalent mass of fibre required are 7.8 g, 15.28 g, 22.29 g and 28.88 g respectively.

### 2.2.3. Development of the Composite

The technique employed in the fabrication of the composite is the compression moulding technique. The method entails the shredding of the polyethylene (pure water sachets) and the subsequent use of plastic recycling machine to form a well-blended mixture of Coir-LDPE (in the desired mix ratio). The low density

polyethylene materials mixed with the coir fibre were fed in through the hopper. The heat from the heater bands and friction & pressure generated along the transition zone of the screw provided the energy needed for the transformation of the materials conveyed to a well-blended molten state. The process was carried out at 175°C. The extrudates were collected from the output end of the machine.

The well-blended Coir-LDPE mixture collected from the plastic recycling machine was then fed into the mould placed on the bed of hydraulic pressing machine. The reciprocating arm was gradually drawn downward by swinging the machine handle until a compressed mixture of the Coir-LDPE composite was obtained. The compression was carried out at the pressure of 10 t (100 kN) for the dwell time of 4 minutes. After the material is cured, the mould is opened and the composite is pushed out.

### 2.2.4. Testing Procedures

#### 1) Tensile Test

The tensile test specimen is prepared according to the ASTM D3039 standard. The testing process involves placing the test specimen in the testing machine and applying tension to it until it fractures. The tensile test of the composites was carried out using Monsanto Tensometer (Type w). The speed of the tensile testing machine was set to 5 mm/min and gauge length of 40 mm. The specimen dimensions were 3 mm thick with a width of 15 mm as shown in **Figure 3**. From this test, the average value of the ultimate tensile strength (UTS), strain ( $\mathcal{E}$ ), elongation at break (% Elongation), and the modulus of elasticity ( $E$ ) for the composites are determined using the following equations respectively.

$$\text{UTS} = \frac{F}{A} \quad (3)$$

$$\mathcal{E} = \frac{\Delta L}{L} \quad (4)$$

$$\% \text{ Elongation} = \frac{\Delta L}{L} \times 100 \quad (5)$$

$$E = \frac{\text{UTS}}{\mathcal{E}} \quad (6)$$

where  $F$  = force, in N;  $A$  = Cross-sectional area, in mm<sup>2</sup>;  $\Delta L$  = change in length, in mm; and  $L$  = gauge length, in mm.

#### 2) Flexural Test

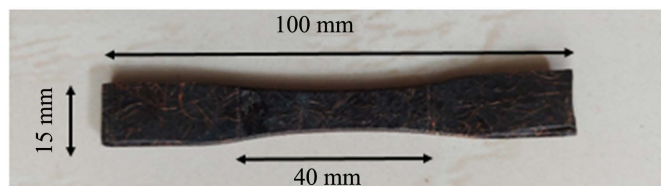


**Figure 3.** Tensile test specimen.

The flexural properties of the composites were measured by a three-point bending method using the same Monsanto Tensometer Machine with load capacity of 5 kN according to D790 standard. The testing process involves placing the test specimen in the testing machine and applying force to it until it fractures and breaks. The flexural tests were carried out at room temperature with a crosshead speed of 3 mm/min. The specimen dimension is 60 × 30 mm as shown in **Figure 4**. The average values of flexural strength ( $\lambda_f$ ) and modulus ( $E_f$ ) of each composite were obtained from four test specimens.

The flexural strength ( $\lambda_f$ ) and the flexural modulus ( $E_f$ ) are given respectively by:

$$\lambda_f = \frac{3FL}{2bd^2} \quad (7)$$

$$E_f = \frac{FL^3}{4bd^3D} \quad (8)$$

where  $F$  = force, in N;  $L$  = gauge length, in mm;  $b$  = width, in mm;  $d$  = thickness/depth, in mm; and  $D$  = deflection, in mm.

### 3) Impact Test

The impact test specimens are prepared according to the required dimension following the ASTM-D256 standard. The charpy impact test is adopted, which measures the energy absorbed by a standard notched specimen while breaking under an impact load. This test consists of striking a suitable specimen with a pendulum while the specimen is held securely at each end. The energy absorbed by the specimen is determined precisely by measuring the decrease in motion of the pendulum arm. The standard charpy impact test specimen dimension of 55 × 10 × 10 mm is adopted as shown in **Figure 5**.

### 4) Water Absorption Test

Moisture absorption test was performed as per ASTM D570 standards. The weight of the samples was taken before subjecting them to normal water. After exposure for 12 hours as shown in **Figure 6**, the specimens were taken out from the moist environment and all surface moisture was removed. The specimens were reweighed to the nearest 0.001 mg; this step was repeated consecutively for 120 hours. The percentage weight gain of the samples was measured at different time intervals by using the following equation:



**Figure 4.** Flexural test specimen.

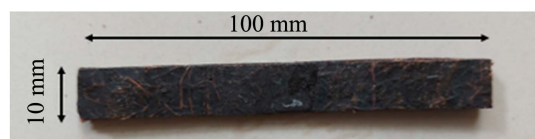


**Figure 5.** Impact test specimen.



**Figure 6.** Water absorption test set up.

$$\%M = \frac{(W_t - W_o) \times 100}{W_o} \quad (9)$$

where  $W_t$  is the weight of specimen at a given immersion time and  $W_o$  is the oven-dried weight.

### 5) SEM Analysis

The microstructural investigation of the moulded composite specimen was carried out to understand the extent of surface fracture when the composite was subjected to flexural testing. In this case, only the test sample containing 40% of fibre was analyzed. This process was done by using Pro X: Phenom at 20.0 kV. To generate the micrograph of the composite sample shown on computer screen as in **Figure 16**.

## 3. Results and Discussion

### 3.1. Mechanical Characterization of the Developed Composites

**Table 1** shows the mechanical properties of the developed composite at different fibre loading.

### 3.2. Effect of Fibre Reinforcement on the Tensile Strength of the Composites

**Figure 7** shows the average modulus of elasticity of the composite at different weight percentages of coir fibre with five percent (5%) error as adopted in [8]. It can be seen that the composite with 20 wt% fibre loading had the highest tensile modulus, while the pure LDPE has the lowest tensile modulus. Also, the incorporation of coir fibre generally improved the modulus of elasticity of LDPE, indicating that the stress is transferred from the LDPE to the stiffer coir fibre.

**Figure 8** shows the average tensile strength of the composite at different weight percentages of coir fibre. It can be seen that the composite with 30 wt% fibre loading had the highest tensile strength, while the pure LDPE has the lowest tensile strength. Although, the tensile strength of the pure LDPE generally increases with the incorporation of coir fibre, this increment trend is randomly distributed as the tensile strength increases with the addition of 10 wt% fibre, decreases at 20 wt% fibre loading and then increases again reaching its peak value of 3.86 MPa at 30 wt% fibre loading. This haphazard trend is attributed to the fact that the tensile

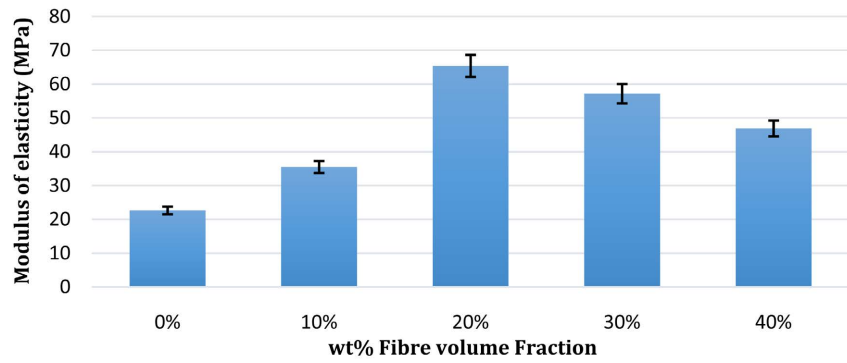


**Figure 7.** Tensile modulus of pure LDPE and Coir-LDPE composites at various fibre loading.

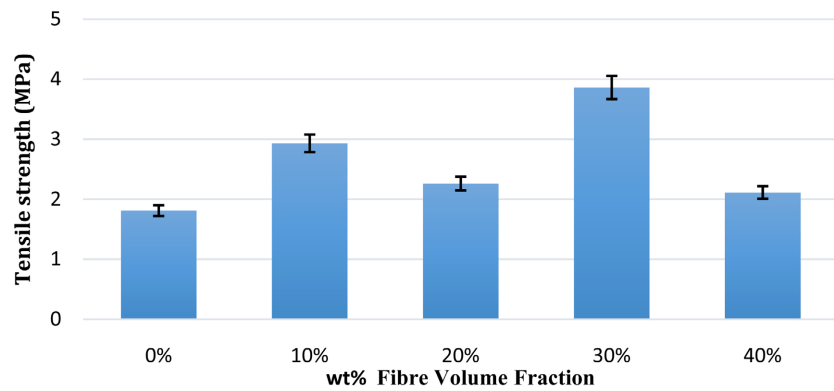


**Figure 8.** Tensile strength of pure LDPE and Coir-LDPE composites at various fibre loading.

**Table 1.** Mechanical properties of the composite at different fibre loading.

Sample	$\lambda_t$ (MPa)	$\epsilon$	$E_t$ (MPa)	$\lambda_f$ (MPa)	$E_f$ (MPa)	$\lambda_i$ (kJ/mm <sup>2</sup> )
0%	1.81	0.08	22.63	6.95	105.6	17.25
10%	2.93	0.0825	35.52	11.15	172.13	18.25
20%	2.26	0.0345	65.38	10.67	193.57	26
30%	3.86	0.0675	57.19	6.81	214.47	28.75
40%	2.11	0.045	46.91	6.54	117.48	14.5

$\lambda_t$  = Tensile strength;  $\lambda_f$  = Flexural strength;  $\lambda_i$  = Impact strength;  $E_t$  = Tensile modulus of elasticity,  $E_f$  = Flexural modulus; and  $\epsilon$  = Strain.

strength is affected by volume fractions, degree of adhesion between the filler and the matrix, level of dispersion of the filler and matrix and surface related defects. This shows similar finding by [9]. The decrease in tensile strength may be explained due to poor wettability leading to a weak interface. In principle, lack of proper wetting between the short fibre and the matrix should lead to the formation of voids at the fibre-matrix interface as shown by [10].



**Figure 9** shows the ductility of pure LDPE and the effect of fibre loading on the ductility of the Coir-LDPE composite in terms of extension per force. It can be observed that the Coir-LDPE composites are less ductile than the pure LDPE which indicates that the fibre loading generally decreases the ductility of the pure LDPE while increasing its stiffness. Consequently, the Coir-LDPE composites withstand higher tensile force before yielding compared to the pure LDPE.

### 3.3. Effect of Fibre Reinforcement on the Flexural Properties of the Composites

The average flexural strength and modulus of Coir-LDPE composite as a function of fibre weight content are presented in **Figure 10** and **Figure 11** respectively. The composite with 10 wt% fibre loading exhibits the maximum flexural strength of 11.15 MPa, while minimum flexural strength of 6.54 MPa at 40 wt% fibre fraction was obtained. Comparing to pure LDPE, the flexural strength of the composite somewhat increases with fibre loading up to 20 wt%, but decreases with upper fibre contents. This may be due to insufficient filling of the melted LDPE resin into the reinforcing natural fibres during composite processing as described by [11].

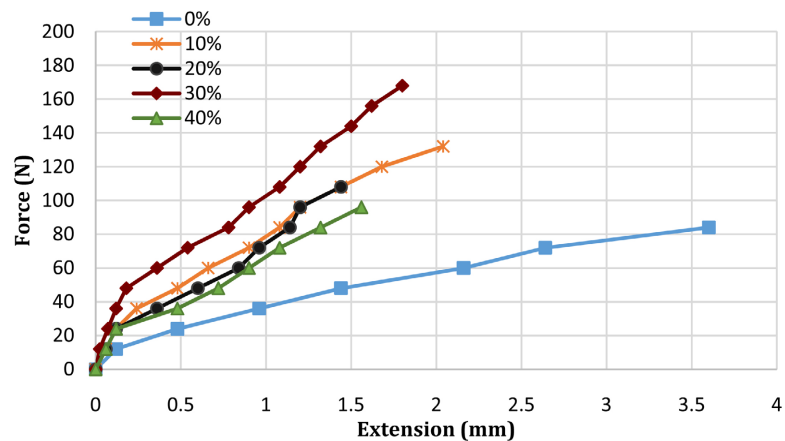


**Figure 9.** Effect of fibre loading on the ductility of the composites.

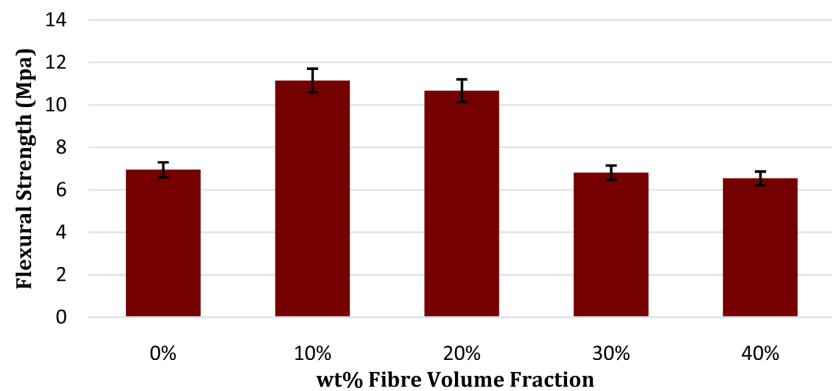


**Figure 10.** Flexural strength of pure LDPE and Coir-LDPE composites at various fibre loading.

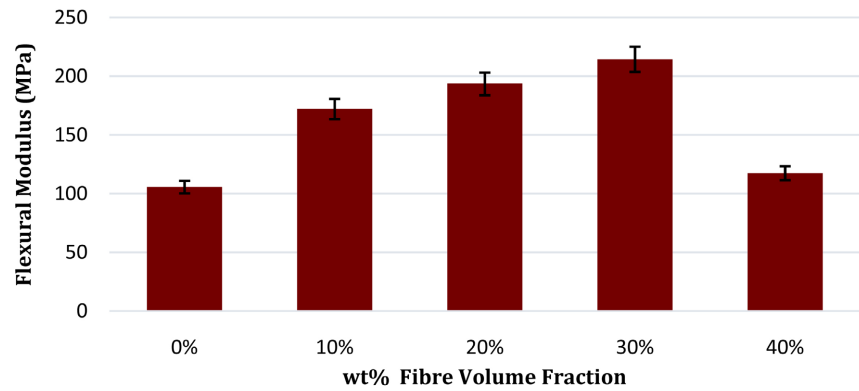


**Figure 11.** Flexural modulus of pure LDPE and Coir-LDPE composites at various fibre loading.

As seen in **Figure 11**, the incorporation of coir fibre generally improved the flexural modulus of the pure LDPE. The greatest flexural modulus of Coir-LDPE composite was obtained with fibre loading of 30 wt%, while the lowest flexural modulus was recorded at 40 wt% fibre loading. The main reason for sudden drop in flexural modulus is the partial filling of matrix in the composites. This shows similar finding by [12].

### 3.4. Effect of Fibre Reinforcement on the Impact Strength of the Composite

**Figure 12** depicts the average value of the impact strength of pure LDPE and various Coir-LDPE composites with varying weight fractions. The Coir-LDPE composite with 30 wt% fibre loading exhibits the highest impact strength of 28.75 kJ/mm<sup>2</sup>. In comparison to the pure LDPE, the incorporation of coir fibre increases the impact strength of the pure LDPE until the fibre loading reaches 40 wt%, where the impact strength of the composite is observed to be at minimum and slightly below the impact strength of pure LDPE.

### 3.5. Locally Average Strength Distribution in the Developed Coir-LDPE Composite

The local strengths of the composites with 10, 20 and 30 wt% fibre loading are evaluated to determine the strength distribution throughout the Coir-LDPE composite developed. The local tensile and impact strengths are examined on a specimen with dimensions of 150 × 100 mm and 60 × 300 mm for flexural strength. Specifically, these strengths are evaluated at an interval of 15 mm and 30 mm, respectively through the specimen along the X-axis.

**Figure 13** shows the local tensile strength distribution in composites with 10, 20 and 30 wt% fibre loading. It can be observed that at 20 and 30 wt% fibre loading, the tensile strength is higher at the center of the specimen and lower at the tip end regions. This can be attributed to the manufacturing method adopted (compression moulding technique). Because during moulding of the composite, it was observed that the resin matrix (LDPE) flowed out of the mould through

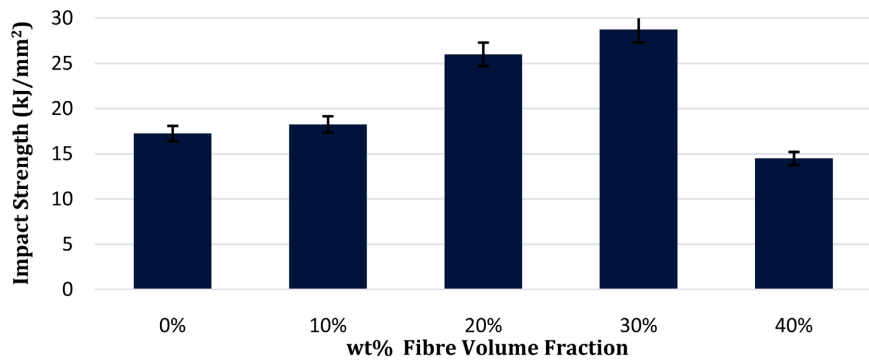


**Figure 12.** Impact strength of pure LDPE and Coir-PE composites at various fibre loading.

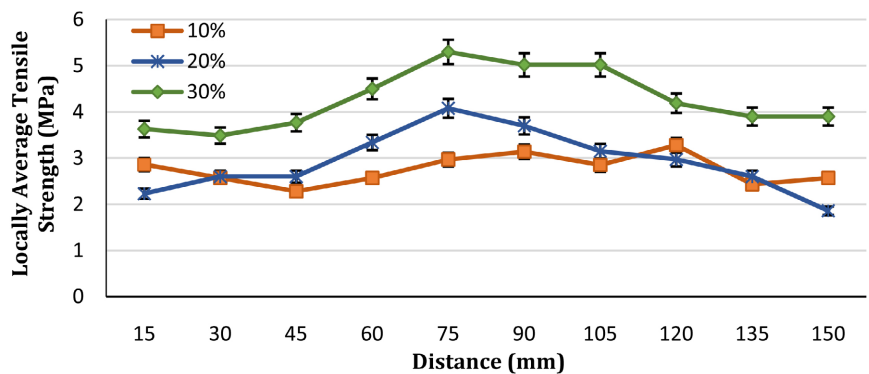


**Figure 13.** Locally average tensile strength distribution in Coir-LDPE composite at different fibre loading.

the gap between the mould and the pressing arm. Consequently, due to this overflow, there is low concentration of matrix at the tip end with high concentration of fibre. Thus, reducing the tensile strength at that region. Hence, the allowance between the mould and pressing arm should be closely controlled where compression moulding is adopted in future works.

**Figure 14** and **Figure 15** show the local flexural and impact strength distribution in composites with 10, 20 and 30 wt% fibre loading, respectively. It can be observed that the flexural strength distribution is almost uniform for Coir-LDPE composite with 10% fibre loading. It can also be seen that at 10 wt% fibre loading, the impact strength is almost uniform in all regions. However, for 20 wt% and 30 wt% fibre loading, the impact strength is lower at the center of the specimen and higher at the tip ends of the specimen. This showed opposite trend to the tensile strength distribution. Hence, it can be concluded that at higher fibre loading (30 wt% and above), the LDPE matrix had more influence on the tensile and flexural strengths of the composites, while the coir fibre had more influence on the impact strength of the composites, all things being equal.

### 3.6. Microstructural Analysis

Morphology of fractured surface of composite with 40 wt% fibre loading is

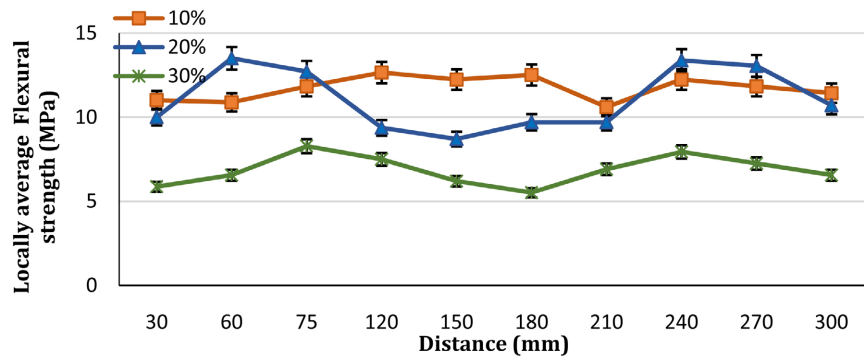


**Figure 14.** Locally average flexural strength distribution in Coir-LDPE composite at different fibre loading.

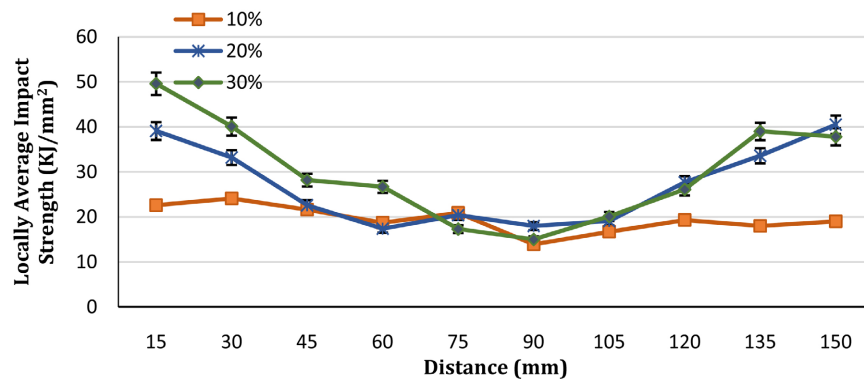


**Figure 15.** Locally average impact strength distribution in Coir-LDPE composite at different fibre loading.

shown in **Figure 16**. It was observed that there is nearly homogenous mixture of the coir fibre and LDPE, indicating that the coir fibre was mixed well with LDPE matrix. As seen in **Figure 16(a)** cracks were observed at the fractured surface which can also be attributed to poor compression of the composites. Aggregation of coir fibre was observed when fibre content reached 40 wt%. However, at 10 wt% and 20 wt% loadings, there is low chance of aggregation as the polyethylene matrix can comfortably accommodate the fibre loading. Also, fibre breakage and fibre pull out were observed at the fractured surface. From **Figure 16(b)**, Gaps were observed between the fibre and the LDPE, which indicate poor interfacial bonding due to poor compression of the composite.

### 3.7. Water Absorption Properties of the Composite

The water absorption behaviours of pure LDPE and the Coir-LDPE composite specimens were measured at room temperature for a maximum period of five days as shown in **Figure 17**. It can be observed that the moisture absorption generally increases with increasing fibre loading. Although, the percentage moisture absorption initially showed considerable rise as the exposure time increases, but there is significant reduction as the immersion time increases. Consequently, the plot of the process of water absorption is linear at the beginning, after which

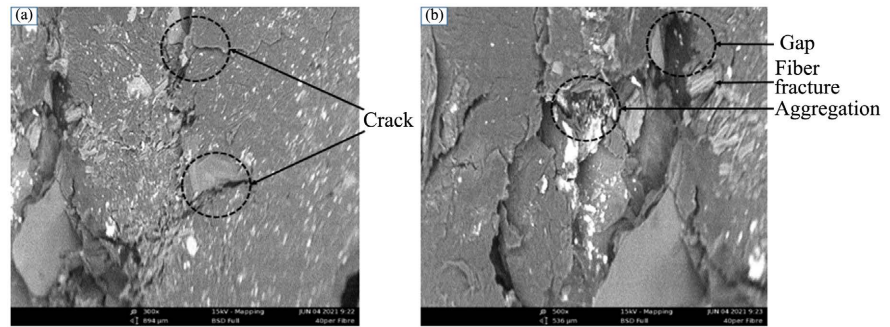


**Figure 16.** SEM micrograph for fractured specimen with 40% fibre loading.

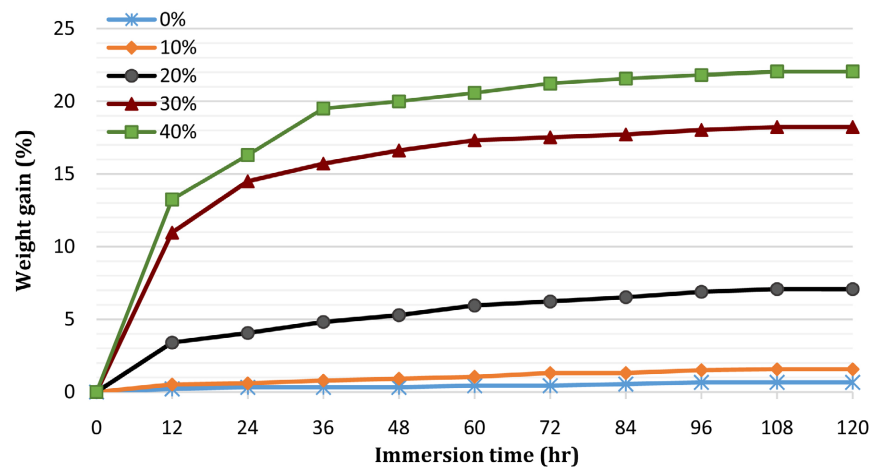


**Figure 17.** Water absorption curves for pure LDPE and Coir-LDPE composites at different fibre loading.

it slows and finally after extended immersion time (about 108 hours), the samples approaches to the saturation stage, where no further water absorption increment was noticed. As seen in **Figure 17**, the water absorbed by pure LDPE was insignificantly small which confirms the hydrophobic nature of polyethylene. Coir-LDPE composite with 40 wt% fibre loading showed the maximum water absorption trend, and this can be attributed to the hydrophilic nature of the coir fibre. Also, specimen swell was observed in the composites with 30 wt% and 40 wt% fibre loading when exposed to the wet environment. This can be attributed to fibre swell and as a result of the fibre swelling, and microcracks are also noticed in the LDPE matrix, which lead to largest transport of water through the fibre matrix interface. Hence, fibre swells and microcracks are the main reason for the significant water absorption by the 30 wt% and 40 wt% coir-LDPE composites as compared to other fibre loading.

#### 4. Conclusions

The application of the compression moulding technique was shown to be a possible way in the development of coconut fibre reinforced low density polyethylene (LDPE) composite material.

Testing and evaluation of the mechanical properties that include: tensile, flexural, and impact strengths were carried out successfully, the results showed that composites with 30 wt% and 20 wt% fibre loading have the most optimum combination of tensile and impact strengths. Unfortunately, the composite with 40 wt% fibre loading that is expected to be at the optimum, exhibit poor properties. This could be based on the high percentage of coir fibre in the mixture, which the resin LDPE cannot adequately bind to produce the better material composition. Therefore, the mixture with 30 wt% is better and within the acceptable limit of the application requirements, especially since flexural strength is rarely encountered in low strength applications.

The microstructure of the developed composite material was captured and investigated. The investigation shows that the fractured surface morphology of composite samples indicated a homogeneous mixture of the coir fibre and the LDPE matrix. Also shown in the microstructure was weak interfacial bonding between the coir fibre and LDPE matrix. This, therefore, concludes that the mixture is adequate and acceptable, even with inadequate bonding.

The moisture absorption rate of the developed composite material was determined. The analysis showed that the developed composite materials have low water absorptivity at low fibre loading and high water absorptivity at higher fibre loading. Also, a thickness swell was observed in the composite with higher fibre loading. Hence, the developed composite is not suitable for in-water applications such as water pipes and marine applications. But it can be applied in moist environments, such as car exteriors and domestic decorations.

The overall conclusion is that the material developed is characterized by low strength compared to synthetic fibre reinforced composites (carbon and glass fibres) shown in literature, but can be applied in lightweight, low strength, or non-structural applications such as panels for partition, false ceiling, roof tiles, window, and door frames.

### Conflicts of Interest

The authors declare no conflicts of interest regarding the publication of this paper.

### References

- [1] Ashby, M.F. and Jones, D.R.H. (1998) *Engineering Materials 2: An Introduction to Microstructures, Processing and Design*. Elsevier, Amsterdam, 239-306.
- [2] Verma, D., Gope, P.C., Shandilya, A., Gupta, A. and Maheshwari, M.K. (2013) Coir Fibre Reinforcement and Application in Polymer Composites: A Review. *Journal of Materials and Environmental Science*, **4**, 263-276.
- [3] Alagarsamy, S., Sagayaraj, A. and Vignesh, S. (2015) Investigating the Mechanical Behaviour of Coconut Coir—Chicken Feather Reinforced Hybrid Composite. *International Journal of Science, Engineering and Technology Research*, **4**, 4215-4221.
- [4] Bazan, P., Nosal, P., Kozub, B. and Kuciel, S. (2020) Biobased Polyethylene Hybrid Composites with Natural Fiber: Mechanical, Thermal Properties, and Microme-

- chanics. *Materials*, **13**, Article 2967. <https://doi.org/10.3390/ma13132967>
- [5] Natsa, S., Akindapo, J. and Garba, D. (2015) Development of a Military Helmet Using Coconut Fiber. *European Journal of Engineering and Technology*, **3**, 55-65.
- [6] Jimoh, Y.A. and Kolo, S.S. (2011) Dissolved Pure Water Sachet as a Modifier of Optimum Binder Content in Asphalt Mixes. *Epistemics in Science, Engineering and Technology*, **1**, 176-184.
- [7] PrakashReddy, B., Satish, S. and Thomasrenald, C.J. (2014) Investigation on Tensile and Flexural Properties of Coir Fiber Reinforced Isophthalic Polyester Composites. *International Journal of Current Engineering and Technology*, **2**, 220-225.
- [8] Hammajam, A.A., El-Jumamah, A.M. and Ismarrubie, Z.N. (2019) The Green Composites: Millet Husk Fiber (MHF) Filled Poly Lactic Acid (PLA) and Degradability Effects on Environment. *Open Journal of Composite Materials*, **9**, 300-311. <https://doi.org/10.4236/ojcm.2019.93018>
- [9] Amulah, C.N., El-Jumamah, A.M. and Modu Tela, B. (2019) Development and Characterization of a Composite Material Based on the Mixture of Gypsum Plaster and Rice Husk Ash. *Continental Journal of Engineering Sciences*, **14**, 15-33.
- [10] Nam, T.H., Ogihara, S., Tung, N.H. and Kobayashi, S. (2011) Mechanical and Thermal Properties of Short Coir Fibre Reinforced Poly (Butylene Succinate) Biodegradable Composites. *Journal of Solid Mechanics and Materials Engineering*, **5**, 251-262. <https://doi.org/10.1299/jmmp.5.251>
- [11] Han, S.O., Lee, S.M., Park, W.H. and Cho, D. (2006) Mechanical and Thermal Properties of Waste Silk Fiber-Reinforced Poly (Butylene Succinate) Biocomposites. *Journal of Applied Polymer Science*, **100**, 4972-4980. <https://doi.org/10.1002/app.23300>
- [12] Karthik, S. and Arunachalam, V.P. (2020) Investigation on the Tensile and Flexural Behavior of Coconut Inflorescence Fiber Reinforced Unsaturated Polyester Resin Composites. *Materials Research Express*, **7**, Article ID: 015345. <https://doi.org/10.1088/2053-1591/ab6c9d>